Journal Name

ARTICLE TYPE

Cite this: DOI: 10.1039/xxxxxxxxxx

Received Date
Accepted Date

DOI: 10.1039/xxxxxxxxxx

www.rsc.org/journalname

Meniscus instabilities in thin elastic layers†

John S. Biggins,‡[a] and L. Mahadevan*[abc]

We consider meniscus instabilities in thin elastic layers perfectly adhered to, and confined between, much stiffer bodies. When the free boundary associated with the meniscus of the elastic layer recedes into the layer, for example by pulling the stiffer bodies apart or injecting air between them, then the boundary will eventually undergo a purely elastic instability in which fingers of air invade the layer. Here we show that the form of this instability is identical in a range of different loading conditions, provided only that the thickness of the meniscus, a, is small compared to the in-plane dimensions and to two emergent in-plane length scales that arise if the substrate is soft or if the layer is compressible. In all such situations, we predict that the instability will occur when the perimeter has receded by approximately $1.27a$, and that the instability will have wavelength $\lambda \approx 2.75a$. We illustrate this by also calculating the threshold for fingering in a thin wedge of elastic material bonded to two rigid plates that are pried apart, and the threshold for fingering when a flexible plate is peeled from an elastic layer that glues the plate to a rigid substrate.

1 Introduction

Interfacial instabilities are commonly associated with fluid-fluid interfaces. The most celebrated examples are Saffman-Taylor fingering[1] when a less viscous fluid invades a more viscous one in a porous media, Rayleigh-Taylor fingering[2,3] when a dense fluid invades a lighter one under the influence of gravity, and the Rayleigh-Plateau instability where a column of fluid breaks into droplets under the influence of its surface tension[4]. More recently, there has been growing interest in the reproduction of these fluid instabilities in soft solids, including direct observations of Rayleigh-Taylor fingers in inverted soft solid slabs[5] and surface tension driven instabilities in soft solid cylinders[6–8]. Here we focus on a range of recent observations of fingering in soft solids[9,10] that are analogous to Saffman-Taylor fingers at the interface of viscous fluids.

Saffman-Taylor fingering has long been explored, experimentally and theoretically, by confining a viscous fluid between two glass plates (a Hele Shaw cell) then injecting a less viscous fluid into it[11]. It is found that the less viscous fluid invades the more viscous fluid via radial finger-like protrusions, with their wavelength set by a competition between surface tension and viscous stress. Recently a soft-solid analogue of this experiment was explored, by pumping air into a cavity in a highly elastic solid layer without fracture or de-adhesion[9]. It was found that at first the cavity simply dilated, but, at a critical pressure, fingers of air invaded the solid layer. Identical fingers have also been seen in elastic layers trapped between rigid bodies if the air is induced to invade the solid layer by pulling the bodies apart while maintaining adhesion[10,12]. In both cases the fingering transition has been observed to be reversible, rate-independent and subcritical.

Elastic layers adhered to rigid bodies arise naturally whenever a soft polymeric glue is used, or when a rubber gasket forms a seal[13]. When fingers of air penetrate such an elastic layer, the peak strain in the elastic layer increases considerably. Although in the experiments detailed above the elastic layers were sufficiently compliant to sustain the necessary strains ($\sim 700\%$) this will not be true of most glues, so in practice fingering is likely to precipitate fracture of the glue and failure of the joint. Elastic fingering is thus a potentially important boundary driven failure mode of glued joints and tight seals.

Many previous studies have examined how the morphology of fluid Saffman-Taylor fingers changes when the fluid properties are changed. Notably, high viscosity contrast and low interfacial tension yields thin fractally branching fingers[14,15], and increasing viscoelasticity is associated with a transition from fingering to fracture[16–23]. Yield stress and shear thinning fluids have also been studied[16,24–27], as have situations in which the fluids react chemically to create an elastic interface[28–30]. However, all of these studies focus on fluids, depending critically on rate-dependent stresses, irrecoverable deformations and surface tension. In contrast, the elastic fingers studied here are completely recoverable and independent of both the rate of loading

[a] Department of Engineering, University of Cambridge, Trumpington St, Cambridge CB2 1PZ, United Kingdom.
[b] School of Engineering and Applied Sciences, and Departments of Organismic and Evolutionary Biology, and Physics, Harvard University, Cambridge, Massachusetts, 02138, USA. E-mail: lmahadev@g.harvard.edu
[c] Kavli Institute for Nanobio Science and Technology, Harvard University, Cambridge, Massachusetts, 02138, USA

and the surface tension, indicating pure elastic behavior.

In the context of solids, four different elastic instabilities have been identified in elastic layers in tension. Three of these arise when an elastic layer adhered between rigid bodies is pulled apart whilst maintaining adhesion. This leads to one of the following: cavitation in the bulk of the elastic layer[31], fingering at the perimeter of the elastic layer[10,12] or an undulating fringe instability localized around the contact line between the layer's perimeter and the the rigid body[32,33]. The fourth tensile instability is entirely different: when adhesion between the layer and the body fails, 2-D patterns of adhered and de-adhered regions emerge on the previously adhered interface from the trade off between adhesive energy and elasticity[34–40]. Which of these instabilities occurs first depends on the aspect ratio of the elastic layer, with cavitation occurring first in very thin layers, fingering in layers of intermediate thickness, and fringing in layers that have an in-plane dimension comparable to their thickness[41]. However, here we show that the key driver for fingering is inward displacement of the layer's perimeter, which can indeed be achieved by pulling apart on the rigid bodies, but can also be achieved, for example, by direct fluid invasion: unlike fringing and cavitation, fingering is not an inherently tensile instability, but rather an invasive instability.

We have previously developed a theoretical framework for understanding the elastic fingering transition based on two approximations. We assume that the displacements in the elastic layer vary quadratically through its thickness, and that the deformations of the elastic layer preserve its volume when averaged through its thickness rather than implementing perfect incompressibility at each point in the layer. These approximations allow us to model the three-dimensional layer with an effective two-dimensional elastic energy which we then minimize. We first used this framework to predict the onset and wavelength of the fingering instability in a minimal rectilinear setting[10]. We have also considered a large annulus shaped elastic layer between rigid glass plates, and predicted elastic fingering on the inner circumference when the plates are pulled apart or when air is pumped into the central cavity, establishing the equivalence of these two superficially different modes of fingering[42].

In this paper we seek to move beyond the very specific geometries treated previously and investigate how general elastic fingering is. We first consider elastic fingering in a generic layer, assuming only that the elastic layer is very thin compared to its in-plane dimensions. We show that if the perimeter of the elastic layer is caused to recede into the layer then it will eventually become susceptible to fingering, and that both the threshold degree of recession and the wavelength of the fingers depend only on the thickness of the layer, not on any other factors pertaining to the morphology of the layer or the loading of the rigid bodies. This shows that the form of the elastic fingering transition is relatively generic.

We illustrate this by considering fingering during the opening a thin elastic wedge and peeling a glued plate from a rigid substrate. Since we have already derived threshold and wavelength results, all that remains to do for these specific geometries is to calculate what degree of loading causes the perimeter of the elastic layer to retreat sufficiently to trigger fingering. The wedge problem is of particular interest because it offers a new perspective on a very old problem[43,44]: typically scientists have worried about the tip of a loaded elastic wedge, but here fingering occurs at the thick end. The peeling problem is noteworthy because we do not treat the substrate as rigid, allowing us to ask how stiff the rigid body needs to be for fingering to occur. We show the bending of the plates introduces a new in-plane length scale, $a^{1/2}(\kappa/\mu)^{1/6}$, where κ is the plates bending modulus, μ the layer's elastic modulus and a its thickness, which quantifies the length-scale over which the plate bends. Fingering follows the universal form provided this length-scale is also large compared to a. Peeling is also of interest because it is a natural geometry for investigating the failure of a glued joint. In the final sections we consider the effects of finite bulk modulus and surface tension on elastic fingering, showing that the former introduces a second in-plane length, $a\sqrt{B/\mu}$, which must also be large compared to a for fingering to follow the universal form, while the latter introduces an elasto-capillary length γ/μ which must be short compared to a for surface tension to remain negligible. We thus ultimately conclude that elastic fingering has a universal form in layers that are thin compared to their in-plane length scales, including $a\sqrt{B/\mu}$ and $a^{1/2}(\kappa/\mu)^{1/6}$, but thick compared to γ/μ. Given the latter scale is typically measured in microns, elastic fingering will have the same form in a wide range of thin but not too-thin layers.

2 Mechanics of meniscus fingering in thin layers

We consider a generic elastic layer with a potentially complex morphology, including varying thickness and curved boundaries, confined between stiff but not necessarily completely rigid bodies. However, we assume that the layer is thin in the sense that all the length scales, $\{l_i\}$, that characterize the the geometry of the layer (for example the layer's in-plane width, the radii of curvature of its boundaries and the length scales over which the thickness changes and over which the rigid bodies flex) are large compared to the thickness of the layer. We then focus our attention on a region at the boundary of the elastic layer that is large compared to its thickness, a, but small compared to all the other length-scales. This smallness means that our region has essentially constant thickness and an essentially straight boundary. We construct a coordinate system based on the boundary so that the elastic layer occupies the region $-a/2 < z < a/2$, $y > 0$ as show in fig. 1.

We next imagine inducing air to invade the elastic layer. There are two ways we might try to achieve this: we can pry apart the stiff bodies, increasing the volume between them and sucking air in, or we can pressurize the air so that it forces its own way in. In either case we assume adhesion is maintained between the elastic layer and the stiff-bodies, so the effect of the invasion of the air is to cause the meniscus to deform, as sketched on the right of fig. 1. If the inward displacement of the central plane of the elastic layer at the boundary is u, we can estimate the strain at the boundary as u/a. The fingering transition, in which the boundary loses stability and invaginates so that fingers of air intrude into

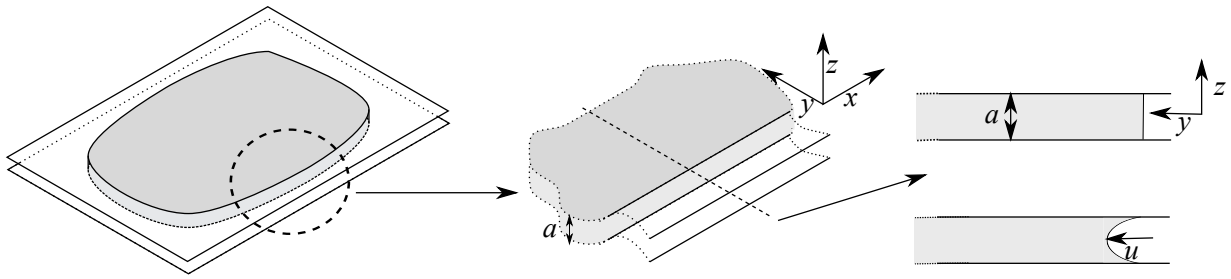

Fig. 1 Sketch of a highly elastic layer (shown in grey) between and adhered to two stiff bodies. We consider a very general case in which the shape of the layer may be any shape, the thickness of the layer may vary and the stiff bodies may bend rather than being completely rigid, but we assume that all of these forms of variation occur over distances much larger than the layer's thickness. We concentrate on a section of the boundary, showed magnified in the middle, which is large compared to the thickness of the layer but small compared to all these other length-scales of variation. In this region the elastic layer has constant thickness a and a single straight boundary. We set up an $x-y-z$ coordinate system on the boundary as shown in the sketch such that the undeformed elastic layer occupied the region $-a/2 < z < a/2$, $y > 0$. Finally, on the right, we sketch a 2-D slice of this magnified region (at constant x). The top figure shows the undeformed layer confined between the stiff bodies. The bottom figure shows the layer after air has been drawn in (for example by very slightly separating the bodies) showing how air invades the layer whilst perfect adhesion is maintained between the layer and the stiff bodies. The displacement u measures how far the perimeter of the layer has retreated.

the layer, is driven by the geometric nonlinearities of large strain elasticity. So we expect it to occur when this strain is of order unity, which is when these non-linearities become important. An immediate consequence of this observation is that we expect any separation of the stiff bodies to be much less than the thickness of the elastic layer. To see this, we note that if the rigid bodies separate by an amount Δa the the change in volume between them is $\Delta a A$, where A is the in-plane area of the layer. As the elastic layer is incompressible, this must equal the volume of air sucked in, which we can estimate as uac where c is the length of the perimeter of the layer. Putting these two results together, we conclude that $\Delta a \sim a^2 c/A \ll a$ at threshold, so that in the limit of a very thin layer, the required separation becomes vanishingly small.

The fingering we seek to describe is an elastic process characterized by the displacement field $\mathbf{U}(x,y,z)$ which records the displacement of each point in the elastic layer. We focus our attention again on the boundary region sketched in fig. 1. We have argued that the displacement of the rigid bodies is very small compared to a so we neglect it completely. Perfect adhesion between the stiff bodies and the layer then requires $\mathbf{U}(x,y,\pm a/2) = 0$. Since this boundary region also has a constant thickness it is symmetric around the $z = 0$ plane. We exploit the thinness and symmetry of the boundary region to expand out its displacement field to second order in z as

$$\mathbf{U}(x,y,z) = (1 - 4z^2/a^2)\mathbf{u}(x,y) \tag{2.1}$$

where $\mathbf{u}$ is the two dimensional in-plane displacement of a point on the central ($z = 0$) plane. Using ∇ as the two dimensional (in the $x-y$ plane) gradient operator and I as the two dimensional identity tensor, we can then write the deformation gradient tensor $F_{ij} = \delta_{ij} + \partial_j \mathbf{U}_i$ as

$$F = I + (1 - 4z^2/a^2)\nabla\mathbf{u} - 8z\mathbf{u}\hat{\mathbf{z}}/a^2 + \hat{\mathbf{z}}\hat{\mathbf{z}}. \tag{2.2}$$

We model the elastic layer as an incompressible neo-Hookean material with an elastic energy density given by $\frac{1}{2}(\mathrm{Tr}\left(F\cdot F^T\right) - 3)$. This energy density can be explicitly integrated in the thickness (z) direction to give an effective two-dimensional elastic energy. To enforce incompressibility we introduce a two dimensional pressure field $P(x,y)$ as a Lagrange multiplier which constrains the thickness averaged volume at each point in the $x-y$ plane. The two-dimensional energy of the elastic layer is then given by

$$L[\mathbf{u},P] = \mu \int_{-a/2}^{a/2} \tfrac{1}{2}(\mathrm{Tr}\left(F\cdot F^T\right) - 3) - P(\mathrm{Det}(F) - 1)\mathrm{d}z \tag{2.3}$$

$$= \mu\left(\frac{2a}{3}\nabla\cdot\mathbf{u} + \frac{4a}{15}\mathrm{Tr}\left(\nabla\mathbf{u}(\nabla\mathbf{u})^T\right) + \frac{8}{3a}\mathbf{u}\cdot\mathbf{u}\right)$$

$$+ \mu a P\left(\frac{2}{3}\nabla\cdot\mathbf{u} + \frac{8}{15}\mathrm{Det}(\nabla\mathbf{u})\right) \tag{2.4}$$

$$= \frac{5\mu a}{6}\left(\frac{1}{2}\mathrm{Tr}\left(G\cdot G^T\right) - 2 + \frac{16}{5}|\mathbf{u}/a|^2 - P(\mathrm{Det}(G) - 1)\right). \tag{2.5}$$

In the above we have introduced an effective two dimensional deformation gradient $G = I + \frac{4}{5}\nabla\mathbf{u}$. We see that the effective two dimensional energy consists of a standard two-dimensional elastic energy and a term that penalizes displacement directly (rather than gradients of displacement), which captures the fact that displacing the central plane of the layer does leads to strain in this problem because the layer is adhered to the boundary at $z = \pm a/2$. We now seek to minimize this energy, so we find the Euler-Lagrange equations for the two fields $\mathbf{u}$ and P:

$$\tfrac{4}{5}a^2\nabla^2\mathbf{u} - \mathrm{Det}(G)\,G^{-T}\cdot a^2\nabla P = 8\mathbf{u} \tag{2.6}$$

$$\mathrm{Det}(G) = 1. \tag{2.7}$$

These Euler-Lagrange equations are augmented by the following natural boundary condition (given by $\partial L/\partial\nabla\mathbf{u}\cdot\hat{n} = 0$ on the boundary)

$$\left(G - P\mathrm{Det}(G)\,G^{-T}\right)_{y=0}\cdot\hat{\mathbf{y}} = 0. \tag{2.8}$$

We next consider the deformation of the elastic layer prior to fingering. This base state is characterized by $\mathbf{u}$ varying over the long length scales associated with the in-plane geometry of the

layer but not on length scales comparable to the thickness of the layer. We therefore Taylor-expand $\mathbf{u}$ around the origin (which is on the boundary) to get

$$\mathbf{u}(x,y) = \left(c_1 + c_2\frac{x}{l_1} + c_3\frac{y}{l_2} + c_4\frac{x^2}{l_3^2} + ...\right)\hat{\mathbf{x}} + \left(d_1 + d_2\frac{x}{l_4} + d_3\frac{y}{l_5} + d_4\frac{x^2}{l_6^2} + ...\right)\hat{\mathbf{y}}, \quad (2.9)$$

where the $\{l_i\}$ are in-plane lengths with $l_i \gg a$. Since the region of the boundary we are focussing on is small compared to all the in-plane lengths, only the zeroth order term in this series is relevant, giving

$$\mathbf{u}(x,y) = c_1\hat{\mathbf{x}} + d_1\hat{\mathbf{y}}. \quad (2.10)$$

With this very simple form for $\mathbf{u}$ we see that $G = I$ and hence that eqn. 2.7 is already satisfied. Solving eqn. 2.6 for P we get

$$P = P_0 - \frac{8c_1x}{a^2} - \frac{8d_1y}{a^2}, \quad (2.11)$$

where P_0 is a constant of integration. We substitute these results into the boundary condition, eqn. 2.8, to get

$$1 - P_0 + \frac{8c_1x}{a^2} = 0, \quad (2.12)$$

from which we conclude that $P_0 = 1$ and $c_1 = 0$, meaning that prior to fingering all displacement near the boundary is perpendicular to the boundary.

The uniform displacement d_1 in the base state casts the term on the right of eqn. 2.6 into a spatially homogeneous force pushing the layer back to zero displacement. The origin of this force is the quadratic profile of the displaced layer, but its effect is exactly analogous to a uniform gravitational field $\rho\mathbf{g}$ pulling the layer back to zero displacement. Furthermore, the stress in the layer rises linearly as one approaches the boundary (eqn. 2.11), just as stress rises linearly with depth under gravity. In general, a sinusoidal perturbation of an interface is associated with a net movement of material along the interface's outward normal. In the gravitational case, this causes a sinusoidal perturbation to release gravitational potential energy so (provided this release outweighs the perturbation's elastic cost) it will grow into Rayleigh-Taylor fingers[5]. Correspondingly, in the confined elastic layer case, a sinusoidal perturbation will generate a net movement of the elastic layer back towards its zero displacement, releasing some of the elastic energy associated with the quadratic displacement profile. If this energy release is larger than the shear elastic energy associated with the distortion, the perturbation will grow and the front will be unstable. Elastic fingering is therefore, mathematically, analogous to Rayleigh-Taylor fingering, although it occurs in physical circumstances reminiscent of Saffman-Taylor fingering.

To determine when such fingering becomes favourable, we now consider the stability of the above base state to fingering by adding an infinitesimal short-wave length perturbation to the base state giving

$$\mathbf{u} = (d_1 + \varepsilon f(y)\cos(kx))\,\hat{\mathbf{y}} + \varepsilon g(y)\sin(kx)\hat{\mathbf{x}} \quad (2.13)$$

$$P = 1 - \frac{8d_1y}{a^2} + \varepsilon h(y)\cos(kx). \quad (2.14)$$

The effective two-dimensional deformation tensor G is now given by

$$G = \begin{pmatrix} 1 & 0 \\ 0 & 1 \end{pmatrix} + \tfrac{4}{5}\varepsilon \begin{pmatrix} g(y)k\cos(kx) & g'(y)\sin(kx) \\ -f(y)k\sin(kx) & f'(y)\cos(kx) \end{pmatrix}. \quad (2.15)$$

The first order correction to the volume conservation equation (eqn. 2.7) is simply

$$g(y) = -\frac{f'(y)}{k}. \quad (2.16)$$

The inverse-transpose of the two-dimensional deformation tensor G is given by

$$\mathrm{Det}(G)\,G^{-T} = \begin{pmatrix} 1 & 0 \\ 0 & 1 \end{pmatrix} + \tfrac{4}{5}\varepsilon \begin{pmatrix} f'(y)\cos(kx) & f(y)k\sin(kx) \\ -g'(y)\sin(kx) & g(y)k\cos(kx) \end{pmatrix}, \quad (2.17)$$

so it is straightforward to expand out the x component of the bulk Euler-Lagrange equation (eqn. 2.6) to first order in ε to get

$$-\tfrac{4}{5}a^2k^2g(y) + \tfrac{4}{5}a^2g''(y) + a^2kh(y) + \tfrac{4}{5}8f(y)kd_1 = 8g(y), \quad (2.18)$$

which, upon substituting for $g(y)$ using eqn. 2.16, can be rearranged to give

$$h(y) = -\frac{4}{5a^2k^2}\left(8d_1k^2f(y) + \left(10 + a^2k^2\right)f'(y) - a^2f'''(y)\right). \quad (2.19)$$

The y component of eqn. 2.6 can also be expanded out to first order in ε, giving

$$-\tfrac{4}{5}a^2k^2f(y) + \tfrac{4}{5}a^2f''(y) - a^2h'(y) + \tfrac{4}{5}f'(y)8d_1 = 8f(y), \quad (2.20)$$

which, upon substitution for $h(y)$ and $g(y)$ (from eqn. 2.16 and 2.19) gives the following fourth order equation for $f(y)$:

$$k^2\left(10 + a^2k^2\right)f(y) - 2\left(5 + a^2k^2\right)f''(y) + a^2f''''(y) = 0, \quad (2.21)$$

subject to stress free boundary conditions (eqn. 2.8) at $y = 0$, and decay conditions at infinity, $f(y \to \infty) \to 0$. We thus initially write f as the sum of the two decaying solutions:

$$f(y) = Ae^{-\frac{\sqrt{10+a^2k^2}y}{a}} + Be^{-ky}. \quad (2.22)$$

To find the constants of integration, (A,B) we expand the stress-free boundary condition, eqn. 2.8, to linear order in ε giving

$$\frac{4}{5}\begin{pmatrix} g'(0) \\ f'(0) \end{pmatrix} - \frac{4}{5}\begin{pmatrix} f(0)k \\ g(0)k \end{pmatrix} - \begin{pmatrix} 0 \\ h(0) \end{pmatrix} = \begin{pmatrix} 0 \\ 0 \end{pmatrix}. \quad (2.23)$$

Substituting our results for f g and h from (2.16), (2.19), (2.22) into the x component of the boundary conditions yields an alge-

braic equations for A/B which we can solve to get

$$\frac{A}{B} = -\frac{a^2k^2}{5+a^2k^2}. \tag{2.24}$$

We can then use the y component of the boundary condition to find the uniform base state of the displacement d_1 in the y direction. Noting that $f'(y) = -kg'(y)$, the equation is equivalent to $8f'(0) = 5h(0)$, or, substituting in for f and h,

$$8 \times Bk\left(\frac{ak\sqrt{a^2k^2+10}}{a^2k^2+5} - 1\right) = 5 \times \frac{8B}{a}\left(\frac{1}{ak} - \frac{4d_1/a}{a^2k^2+5}\right). \tag{2.25}$$

Solving for d_1, the threshold for instability is then:

$$\frac{d_1}{a} = \frac{25+a^2k^2\left(10+ak\left(ak-\sqrt{10+a^2k^2}\right)\right)}{20ak}. \tag{2.26}$$

Finally, we minimize this threshold over k to discover the wavelength and threshold of the first unstable fingering mode. The first unstable mode has a wavelength ($\lambda = 2\pi/k$) of

$$\lambda = 2.74601....a \tag{2.27}$$

and occurs at a threshold value of d_1

$$d_1 = 1.26756...a. \tag{2.28}$$

We recall that the coefficient d_1 corresponds to the displacement of points on the boundary of the elastic layer half way between the stiff bodies. The above calculation reveals any mechanism designed to draw air into a thin confined elastic layer will first cause the layer to retract homogeneously normal to the boundary and then, when the layer has retracted by $1.27...a$, fingers of air with a wavelength of $2.74...a$ will protrude into the layer.

3 Meniscus fingering in opening wedges

The universal geometric form for elastic fingering (including wavelength, threshold retraction etc) established in section 2, applies whenever a confined layer retracts, provided only that the layer is thin. This thinness requirement allows both the confinement geometry and base-state retraction to vary in-plane, provided they do so on length-scales long compared to a, the boundary layer thickness. Our first example of this general form, is the opening of a thin wedge-shaped elastic layer confined between rigid plates. The initial angle of the elastic wedge is 2α and the layer is perfectly adhered to the two plates. Air is then drawn into the layer by opening the angle between the plates to $2(\alpha+\delta\alpha)$, as sketched in fig. 2. The general requirement of layer-thinness here means the wedge angle must be small, $\alpha \ll 1$, so that, for example, the layer thickness varies very little within the finger-forming region at the open end of the wedge. Using an $r-\theta-z$ coordinate system (as shown in fig. 2) the elastic layer initially occupies the region $r < l$, $-\alpha < \theta < \alpha$.

After deformation the point in the elastic layer at (r,θ,z) is moved to $(R(r,\theta,z),\Theta(r,\theta,z),Z(r,\theta z))$. In a thin wedge θ is the thickness coordinate so we expand out these fields to second order in θ. We impose symmetry under $\theta \to -\theta$ and that $R(r,\pm\alpha,z) = r$,$Z(r,\pm\alpha,z) = z$ and $\Theta(r,\pm\alpha,z) = \pm(\alpha+\delta\alpha)$ to maintain perfect adhesion between the layer and the plates, giving

$$R(r,\theta,z) = r + (1-(\theta/\alpha)^2)u_r(r,z) \tag{3.29}$$

$$\Theta(r,\theta,z) = \frac{\alpha+\delta\alpha}{\alpha}\theta \tag{3.30}$$

$$Z(r,\theta,z) = z + (1-(\theta/\alpha)^2)u_z(r,z). \tag{3.31}$$

The general form for the deformation gradient, F, in polar coordinates (after a rigid body rotation that ensures the reference and target points have $\theta = \Theta$) is

$$F = \begin{pmatrix} \frac{\partial R}{\partial r} & \frac{1}{r}\frac{\partial R}{\partial \theta} & \frac{\partial R}{\partial z} \\ R\frac{\partial \Theta}{\partial r} & \frac{R}{r}\frac{\partial \Theta}{\partial \theta} & R\frac{\partial \Theta}{\partial z} \\ \frac{\partial Z}{\partial r} & \frac{1}{r}\frac{\partial R}{\partial \theta} & \frac{\partial Z}{\partial z} \end{pmatrix}. \tag{3.32}$$

We again formulate a two dimensional effective energy for the elastic layer by modeling the layer as a neo-Hookean solid with thickness (θ) averaged volume preservation, leading to the effective energy

$$L = \mu\int_{-\alpha}^{\alpha}\tfrac{1}{2}\left(\mathrm{Tr}\left(F\cdot F^T\right)-3\right) - P(\mathrm{Det}(F)-1)r\mathrm{d}\theta, \tag{3.33}$$

which is directly analogous to eqn. 2.3. We could, with significant algebraic difficulty, determine the onset of wavelength of fingering in this system by substituting the quadratically varying fields (eqns. 3.29-3.31), explicitly conducting the above θ integral to produce a two-dimensional energy, finding the Euler-Lagrange equations and boundary conditions for the new energy and then, under the assumption that the layer is thin, conducting a stability analysis on these equations. However, in the light of the results in the previous section we see that we only need to treat the "base-state" to see what separation of the plates, $\delta\alpha$, will lead to sufficient retraction of the layer to drive fingering. We therefore restrict our attention to fields that are translationally invariant in the z direction, giving

$$u_r(r,z) = u_r(r) \tag{3.34}$$

$$u_z(r,z) = 0, \tag{3.35}$$

which simplifies F to

$$F = \begin{pmatrix} \left(1-\frac{\theta^2}{\alpha^2}\right)u_r'(r)+1 & -\frac{2\theta u_r(r)}{\alpha^2 r} & 0 \\ 0 & \frac{(\alpha+\delta\alpha)}{\alpha}\left(1+\left(1-\frac{\theta^2}{\alpha^2}\right)\frac{u_r(r)}{r}\right) & 0 \\ 0 & 0 & 1 \end{pmatrix}. \tag{3.36}$$

Furthermore, the form of the field $u_r(r)$ is completely determined by the constraint that the thickness averaged volume be preserved (which would be the Euler-Lagrange equation given by varying the pressure in the original energy). This constraint is simply

$$\int_{-\alpha}^{\alpha}(\mathrm{Det}(F)-1)r\mathrm{d}\theta = 0, \tag{3.37}$$

which, upon substituting the above form for F gives

$$15\delta\alpha r + 2(\alpha+\delta\alpha)\left((4u_r(r)+5r)u_r'(r)+5u_r(r)\right) = 0. \tag{3.38}$$

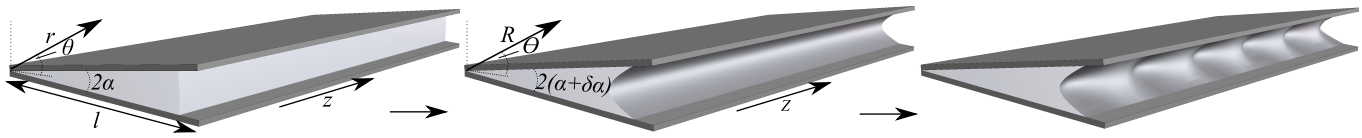

Fig. 2 Sketch of a highly elastic layer (light grey) between and adhered to two rigid plates (dark grey) in a wedge shape. On the left is the unstrained state, labeled with coordinates (r,θ,z), in which the elastic layer occupies the region $-\alpha<\theta<\alpha$ and $r<l$. In the middle is the base deformation state, labeled with coordinates (R,Θ,Z), in which the plates have been opened to make an angle of $2(\alpha+\delta\alpha)$, drawing air into the elastic layer. At a critical value of $\delta\alpha$ fingers of air will protrude into the layer along the $r=l$ boundary, as sketched on the right.

This has two solutions for $u_r(r)$ of the form,

$$u_r(r)=\frac{1}{4}\left(-5r\pm\sqrt{\frac{A+5r^2(5\alpha-\delta\alpha)}{\alpha+\delta\alpha}}\right), \tag{3.39}$$

where A is a constant of integration. Perfect adhesion at the point $r=0$ requires that $u_r(0)=0$, which sets $A=0$. The requirement that if $\delta\alpha=0$ then there should be no displacement, so $u_r(r)=0$, requires us to choose the solution

$$u_r(r)=\frac{1}{4}r\left(-5+\sqrt{-5+\frac{30\alpha}{\alpha+\delta\alpha}}\right). \tag{3.40}$$

Inspecting the form of the quadratic fields, (eqns. 3.29-3.31), we see that $u_r(r)$ represents the displacement in the r direction of a point on the central ($\theta=0$) plane of the wedge. If the wedge has total length l then the thickness of the wedge at its fat-end is $2\alpha l$. We know from the previous section that the onset of fingering will occur when $u(l)=-1.27...2\alpha l$,which given us the expression

$$\frac{1}{4}\left(-5+\sqrt{-5+\frac{30\alpha}{\alpha+\delta\alpha}}\right)=-1.27...\times 2\alpha. \tag{3.41}$$

If we expand this out for small $\delta\alpha$ we discover that

$$\delta\alpha=3.38015...\alpha^2. \tag{3.42}$$

Provided the wedge is thin (i.e. $\alpha\ll 1$) this is indeed very small, making the expansion self-consistent. We see, as expected, that the critical degree of opening depends only on the initial angle of the wedge and that, for thin wedges, the required degree of opening to trigger fingering becomes is negligible compared to the thickness of the wedge. We also note that we can also express the wavelength of the instability in terms of the parameters of the wedge as

$$\lambda=2.74601....\times 2\alpha l=5.49202...\times\alpha l. \tag{3.43}$$

In thicker wedges, fingering is still expected, but will no-longer follow the universal form, as the elastic fields associated with the fingers, which are localized to the open-end of the wedge, will never-the-less "feel" the diminishing layer thickness and retraction towards the wedge's tip. In this case, fingering is expected to morph into a "fringing" form, with separate undulations at the top and bottom plates of the wedge[32,33].

4 Meniscus fingering when peeling glued plates

Next we consider a thin elastic layer between a completely rigid substrate and a stiff (but somewhat flexible) plate. We then consider trying to lift one end of the plate. This geometry models a plate glued to a rigid substrate, with the elastic layer modeling the glue. Lifting one end of the plate corresponds to trying to peel the plate off the substrate, as sketched in fig. 3. As with the wedge geometry, the peeling action increases the volume between the plate and the substrate causing the boundary of the elastic layer to retreat, which will ultimately lead to fingers of air invading the layer at the boundary. This geometry resembles previous work on peeling plates from soft elastic layers,[35–37,39,40], but with the very significant difference that in this case adhesion is maintained, while the previous studies focussed on the movement of the contact line between layer and plate caused by de-adhesion and were in a linear-elastic regime.

The peeling problem is more complicated than the wedge problem because the plate is not perfectly rigid, so when we lift its end up we do not a-priori know what shape it will adopt. To model this situation we take our elastic layer to initially occupy the region $0<z<a$, $y>0$ and to be perfectly adhered to a rigid substrate at $z=0$ and to the plate, which is initially at $z=a$. We then imagine lifting the end of the plate so that the point on the plate initially at (x,y,a) moves to $(x,y,a+h(y))$. Our assumption that the plate only moves in the z direction will be justified provided that $h'(y)\ll 1$ because, since the initial state of the plate is flat, the change to its length caused by this form of deformation is second order in $h'(y)$.

As in our previous examples, we expand the displacements of the point in the elastic layer at (x,y,z), $\mathbf{U}(x,y,z)$, to leading order in z and impose the condition of perfect adhesion between the layer and the rigid substrate (at $z=0$) and the plate (at $z=a$) giving:

$$\mathbf{U}(x,y,z)=4\frac{z(a-z)}{a^2}\mathbf{u}(x,y)+\frac{z}{a}h(y)\hat{\mathbf{z}}, \tag{4.44}$$

where, as in our general treatment, $\mathbf{u}(x,y)$ is a two-dimensional vector in the $x-y$ plane corresponding to the $x-y$ displacement of a point in the elastic layer at $(x,y,a/2)$. We note that the in-plane displacement has a symmetry around $z=a/2$, which is perhaps unexpected given the lack of symmetry between the layer's top and bottom in this geometry. If $h(y)=h_0$ were constant, this symmetry would be self-evident, as the problem would be equivalent to displacing the top and bottom symmetrically by $\pm h_0/2$.

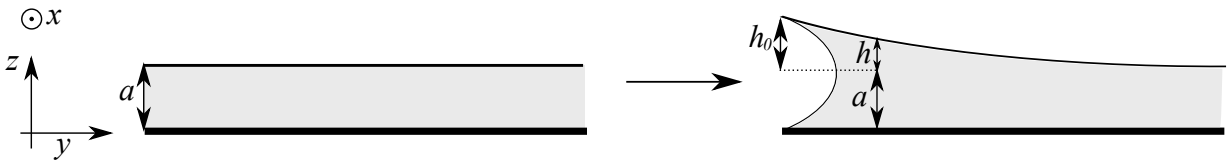

Fig. 3 A thin elastic layer (grey) between a completely rigid substrate (thick black line, bottom) and a stiff (but somewhat flexible) plate (black line, top). On the left is the configuration of plate and layer before any deformation, with the layer occupying the region $y>0$, $0<z<a$ and the plate in a flat configuration at $z=a$. On the right is the situation after the ($y=0$) end of the plate has been lifted by an amount h_0. Consequently the plate at y has lifted by an amount $h(y)$ and air has been drawn into the elastic layer at the $y=0$ boundary. Fingers of air will eventually invade the layer at this boundary.

Thus, any asymmetry arrises via in-plane variation of h, and will be negligible (higher-order) given $h'(y)\ll 1$. This displacement defines a deformation gradient $F=\delta_{ij}+\partial_j \mathbf{U}_i$ which, using ∇ as the in-plate $(x-y)$ gradient operator and I and the in-plane $(x-y)$ identity matrix, we can write as

$$F = I + \frac{4z(a-z)}{a^2}\nabla\mathbf{u} + \frac{4(2z-a)}{a^2}\mathbf{u}\hat{\mathbf{z}} + (1+h/a)\hat{\mathbf{z}}\hat{\mathbf{z}}. \tag{4.45}$$

As in our previous examples, we model the elastic layer as neo-Hookean and add to the elastic energy a two dimensional pressure field $P(x,y)$ to implement the thickness (z) averaged volume preservation. However, in this case our elastic energy for the layer is supplemented by an energetic penalty for bending the plate, which we estimate as $\frac{1}{2}\kappa h''(y)^2$ per unit area of the plate, where κ is the bending modulus of the plate. This leads us to the full two-dimensional effective energy

$$L = \mu\int_0^a \tfrac{1}{2}(\mathrm{Tr}\left(F\cdot F^T\right)-3) - P(\mathrm{Det}(F)-1)\mathrm{d}z + \tfrac{1}{2}\kappa h''(y)^2. \tag{4.46}$$

As with the wedge-case, we can simplify our analysis considerably by restricting attention to the "base-state" deformations prior to fingering. In this case we expect translational symmetry (in the x direction) to be maintained, so that

$$P(x,y) = P(y) \tag{4.47}$$

$$\mathbf{u}(x,y) = u_y(y)\hat{\mathbf{y}}. \tag{4.48}$$

Unfortunately, even after focussing on these one-dimensional fields, the Euler-Lagrange equations for L are too non-linear to admit a closed solution. However, we can make progress by assuming that the plate is very much stiffer than the elastic layer, and hence the displacement of the plate decays over a length l that is much much greater than the thickness of the elastic layer, that is $l\gg a$. This regime of a base-state varying slowly in plane, is, in any event, required for fingering to adopt the universal form. We know that at threshold the displacement of the elastic layer $u_y\sim a$. We also know from volume conservation in the elastic layer that $hl\sim u_y a$, so we can estimate that $h\sim u_y\times(a/l)\sim a^2/l$. We therefore rewrite $h(y)$ and $u_y(y)$ as

$$u_y(y) = a\tilde{u}_y(y/l) \tag{4.49}$$

$$h(y) = \frac{a^2}{l}\tilde{h}(y/l), \tag{4.50}$$

where $\tilde{u}_y$ and $\tilde{h}$ are both dimensionless functions which, at threshold, are of order 1. Furthermore, since these dimensionless functions also have rescaled arguments, y/l, at threshold they decay over an interval $y/l\sim 1$, and thus also have order 1 derivatives. We can now expand each term in the energy as a series expansion in the dimensionless small parameter a/l and identify the terms which dominate when the layer is thin. The first (neo-Hookean) term evaluates to

$$\int_0^a \tfrac{1}{2}(\mathrm{Tr}\left(F\cdot F^T\right)-3)\mathrm{d}z = a\left(\frac{8}{3}\tilde{u}_y\left(\frac{y}{l}\right)^2 + \mathscr{O}\left(\frac{a}{l}\right)\right), \tag{4.51}$$

while the constraint term evaluates to

$$\int_0^a (\mathrm{Det}(F)-1)\mathrm{d}z = a\left(\frac{a}{l}\left(\tilde{h}\left(\frac{y}{l}\right)+\frac{2}{3}\tilde{u}_y'\left(\frac{y}{l}\right)\right)+\mathscr{O}\left(\frac{a^2}{l^2}\right)\right). \tag{4.52}$$

We see that for these terms to be relevant in the energy we expect $P\sim l/a$. Returning to our original variables, we can therefore write the energy to leading order as

$$L = \mu a\left(\frac{8u_y(y)^2}{3a^2} - P(y)\left(\frac{h(y)}{a}-\frac{2}{3}u_y'(y)\right)\right) + \frac{1}{2}\kappa h''(y)^2. \tag{4.53}$$

The Euler-Lagrange equations for the three fields, u_y, h and P are:

$$8u_y(y) + a^2P'(y) = 0 \tag{4.54}$$

$$\mu P(y) - \kappa h''''(y) = 0 \tag{4.55}$$

$$3h(y) + 2au_y'(y) = 0. \tag{4.56}$$

These bulk-equations are augmented by the boundary condition $h(0)=h_0$, which encodes that the end of the plate has been lifted a distance h_0, and $h'(x), h''(x), h'''(x)$ decaying far from the meniscus. Minimization of the energy with respect to $u_y(0)$ and $h'(0)$ leads to the additional natural boundary conditions $\partial L/\partial u_y'\big|_{y=0} = 0$ and $\partial L/\partial h''\big|_{y=0}=0$, so the full set of boundary conditions are:

$$h(0) = h_0, \tag{4.57}$$

$$P(0) = 0, \tag{4.58}$$

$$h''(0) = 0. \tag{4.59}$$

We can straightforwardly eliminate $P(y)$ and $u_y(y)$ from the bulk

equations, yielding a sixth-order linear equation for $h(y)$:

$$12h(y) = \frac{a^3\kappa}{\mu}h^{(6)}(y). \tag{4.60}$$

This equation has solutions which decay with characteristic length $l = \left(a^3\kappa/\mu\right)^{1/6}$[35]. Using this length-scale, and imposing the condition $h(y) \to 0$ as $y \to \infty$, the solution is

$$h(y) = c_1 \exp\left(-\frac{2^{1/3}3^{1/6}y}{l}\right) + \left(c_2\cos\left(\frac{3^{2/3}y}{2^{2/3}l}\right) + c_3\sin\left(\frac{3^{2/3}y}{2^{2/3}l}\right)\right)\exp\left(-\frac{3^{1/6}y}{2^{2/3}l}\right), \tag{4.61}$$

where c_1, c_2 and c_3 are undetermined constants. Imposing the boundary conditions (eqns. 4.57-4.59) on this solution yields

$$c_1 = h_0/3 \tag{4.62}$$

$$c_2 = 2h_0/3 \tag{4.63}$$

$$c_3 = 0, \tag{4.64}$$

and allows us (via the remaining Euler-Lagrange equations) to easily determine the full base-state fields $h(y), u_y(y), P(y)$, where the field $u_y(y)$ is the displacement (in the y direction) of the central $z = a/2$ plane of the elastic layer. The threshold for fingering is, as always, $u_y(0) = 1.27...a$, which then allows us to find the required displacement of the plate

$$h_0 = 1.9179...\frac{a^2}{l} = 1.9179...a^{3/2}\left(\frac{\mu}{\kappa}\right)^{1/6}. \tag{4.65}$$

We note that the three functions u_y, P, and h are all functions of y/l with the expected magnitude at threshold, indeed the main result of the calculation is to identify this long length-scale as $l = \sqrt{a}(\kappa/\mu)^{1/6}$. The terms we neglected in L will indeed be negligibly small provided $l \gg a$. It is important that our linearization of the energy in a/l does not in any way assume the strains in the layer are small compared to one, indeed the strains in the layer are of order one at threshold. Also, if we were to continue our treatment of this problem and conduct a stability analysis, additional terms in the energy would become important because the oscillatory perturbations vary over a length-scale a rather than l, so their derivatives are not smaller by factors of l.

5 Role of compressibility and capillarity

Soft rubbers typically have bulk moduli more than a million times higher than their shear modulus, so the assumption of incompressibility is generally an excellent approximation. An infinite bulk-modulus makes the elasticity of a confined layer infinitely long-ranged as a change in volume introduced at one point (for example by injecting air into a cavity) must propagate to the boundary rather than being mitigated by the material around the cavity changing volume. However, elastomers are not perfectly incompressible, meaning the effects of an imposed volume change are localized, albeit with a long length-scale.

Here we crudely estimate this long-length scale by considering a thin-strip shaped elastic layer occupying the region $-a/2 < z < a/2$, $-l < y < l$, with $l \gg a$, and adhered to flat rigid plates at $z = \pm a/2$. The flat plates are then separated by an additional distance Δa. If the above elastic layer is perfectly incompressible then volume conservation requires that the inward displacement of a point with coordinates y and $z = 0$ be $u \sim \Delta a y/a$, and therefore that it suffer a strain $\gamma \sim u/a \sim \Delta a y/a^2$ and has an energy density $\mu\left(\Delta a y/a^2\right)^2$. If the layer instead deformed by simply increasing its volume, its fractional volume change would simply be $\Delta a/a$, leading to an energy density $B(\Delta a/a)^2$, where B is the elastomers bulk modulus. Equating these two energy densities, a characteristic long in-plane distance emerges $l_2 \sim a\sqrt{B/\mu}$, which is the distance over which the layer behaves in an incompressible way. In the above strip geometry, we expect that if the width of the strip, $l \gg l_2$ then the central portion of the strip will respond to the separation of the plates by increasing its volume, while only the parts of the layer within l_2 of the boundaries will deform in an incompressible way. From the perspective of causing the boundary of the elastic layer to retreat to drive fingering at the boundary, the effective with of the strip is therefore reduced to l_2. This provides an additional in-plane length scale that must be large compared to the thickness of the layer for fingering to proceed along the lines sketched in section 2.

Real elastic layers also have a finite surface tension γ, requiring us to add a surface energy γA to the elastic energy, where A is the area from the elastic layer's perimeter. The elastic strains associated with finger formation are of order one and are localized to distances of order a of the layer's perimeter, so the change in elastic energy per unit length of boundary is of magnitude $E_{el} \sim \mu a^2$, while the corresponding surface energy has magnitude $E_{cap} = \gamma a$. Thus surface tension becomes energetically relevant if $a \leq \gamma/\mu$, a length scale known as the elasto-capillary length. Our surface-tension free theory therefore requires that, in addition to the thickness of the layer being small compared to the previously discussed in-plane length-scales (i.e. that the layer be geometrically thin) it must also be thick compared to the elasto-capillary length-scale. Surface tensions in soft materials are typically of magnitude $\gamma \sim 10^{-2}\mathrm{Jm}^{-2}$ so, even for layers with elastic moduli of $\mu \sim 500\mathrm{Pa}$, the elasto-capillary length is at most a few tens of microns, meaning surface tension will only become relevant in the very thinnest and softest of layers. Our surface-tension free theory thus has a wide range of validity.

6 Conclusions

It has been established in previous publications that if an elastic layer is adhered above and below to rigid bodies and then air is induced to invade the elastic layer (either by separating the rigid bodies to suck air in or by injecting air into a cavity in the layer) then, after a threshold, fingers of air will invade the layer along the boundary. However, previous treatments of this problem have been for very specific geometries. In this paper we have shown that the phenomenon is universal, provided that the layer is geometrically thin, that is, its in-plane length-scales l_i are all large compared to the thickness a of the layer, then attempting to draw air into the layer will result in fingering at the boundary. Further-

more, the fingering will follow an essentially universal form: the wavelength of the fingers will be the same multiple of the thickness of the layer in all systems, $\lambda \approx 2.74a$, and will occur when the invading air has caused the boundary to retreat by a universal multiple of of the thickness of the layer, $u \approx 1.26a$. We have also outlined a general method for treating fingering problems in thin elastic layers, the essential idea being that we only need to find the "base-state" deformations (those prior to fingering), and then apply our universal criteria for the onset and wavelength of fingering to this base-state. We have illustrated this procedure by calculating the onset of fingering in two more complex geometries: opening an elastic wedge and peeling a stiff plate.

Our peeling geometry is reminiscent of a thin plate glued to a rigid substrate, with the glue being our elastic layer. The peeling then corresponds to trying to de-adhere the plate from the substrate. Our threshold for how far the end of the plate must be lifted before fingering takes place is $h_0 \approx 1.92...a^{3/2}\left(\frac{\mu}{\kappa}\right)^{1/6}$, which is further for less rigid plates. However, we can estimate the bending energy of the plate (per unit length in the x direction) as $E_b \sim \frac{1}{2}\kappa(h/l_1^2)^2 l_1$. We expect this to be of similar magnitude to the energy of the elastic-layer since l_1 is chosen to minimize the sum of these two contributions. The derivative of this energy with respect to h tells us the force (per unit distance) required to lift the end of the plate a distance h, $F_h \sim h\kappa/l_1^3$. Evaluating this estimate at h_0 we see that the force required to trigger fingering is $F_{h_0} \sim \kappa^{1/3}\mu^{2/3}$. Therefore, although stiffer plates require less displacement to trigger fingering they require more force.

Our conclusion that elastic fingering in these layers has a general form is subject to three important caveats. In addition to the layer being thin in the sense that its in-plane geometric parameters must be large compared to its thickness, there are two "hidden" in plane length-scales that must also be large. The first emerges if the rigid bodies that the layer is trapped between are not perfectly rigid but instead have a large but finite bending modulus κ, and is the length-scale over which the bodies then bend, given by

$$l_1 = \sqrt{a}\left(\frac{\kappa}{\mu}\right)^{1/6}. \tag{6.66}$$

The second "hidden" length-scale arrises if the elastic layer is not perfectly incompressible but has large bulk modulus B, and is the length-scale over which bulk-deformations become energetically preferable to shear deformations, given by

$$l_2 = a\sqrt{\frac{B}{\mu}}. \tag{6.67}$$

The condition $l_2 \gg a$ is not at all difficult to achieve. For a soft rubber, we can easily have $B/\mu > 10^6$, making $l_2/a \sim 1000$. However, for the very thin layers arising when soft polymeric glues are used, l_2 could easily be rather shorter than the geometric size of the layer, meaning it will be important in determining the separation required to induce fingering. In contrast, $l_1 \gg a$ is a more rigorous constraint. If the elastic modulus of the stiff bodies is μ_p and they have thickness t we expect $\kappa \sim t^3\mu_p$, giving $l_2 \sim \sqrt{at}(\mu_p/\mu)^{1/6}$. The weak dependence on μ_p in this length-scale means that it is very challenging to make this length long by making the rigid bodies out of a stiff material. However, this length-scale can easily be made long by taking thick bodies with large values of t.

The third caveat also relates to a "hidden" length scale, the elasto-capillary length

$$l_{cap} = \frac{\gamma}{\mu}. \tag{6.68}$$

However, in this case the layer must be *thick* compared to l_{cap}, otherwise surface-tension effects become important, and the fingering transition will change accordingly. This is also a weak constraint since, for most soft materials, we expect l_{cap} to be a few microns. However, with very soft thin layers, the regime with $a \sim l_{cap}$ is surely experimentally accessible.

Finally, we note that there are several outstanding challenges in this area. The first is to prove that the transition to the fingered state is subcritical. This was shown experimentally and numerically[9,10] but has not yet been treated analytically. Secondly, we speculate that at very small thicknesses surface tension may become important, as it is in Saffman-Taylor viscous fingering, which may modify our purely elastic results. In the analogous Saffman-Taylor fluid problem, surface tension promotes stability, and the same might naively be expected in the elastic case since the formation of large fingers surely increases the interfacial area. However, surface-tension can also drive instability, most famously in the undulating instability of fluid or solid columns[4,6,7], known as the Rayleigh-Plateaux instability. In these cases surface tension drives instability because undulatory perturbations to a cylinder can reduce its area while preserving its volume, so the instability reduces the surface energy. In the elastic fingering case, as the boundary recedes prior to fingering, it becomes highly curved in the thickness direction, having a shape reminiscent of a half-cylinder. We might similarly expect finger-like undulating perturbations to the boundary to decrease its area, and hence surface tension to help destabilize the boundary. Which of these competing intuitions is correct is a promising topic for further work.

Finally, glued joints typically fail via stress induced instabilities. Two main categories of failure have been studied: bulk failure of the glue via cavitation or fracture, and direct adhesive failure at the boundary between the glue and the substrate. However, our analysis suggests that stress in a layer of glue under tension tends to be very high at the perimeter of the glue, and that this leads to a fingering instability at the perimeter. Fingering is also a failure mode for elastic seals when they are invaded by the fluid they are intended to contain, generating a leak[13]. We speculate that there is a third category of failure modes for glued joints initiated at the perimeter of the glued layer by elastic fingering. Experimental verification of these failure modes and understanding how to control them would make elastic fingering a problem of some practical importance.

References

1 P. Saffman and G. Taylor, *Proc. R. Soc. Lond. A.*, 1958, **245**, 312–329.

2 J. L. R. Strutt, *Proc. Lond. Math. Soc.*, 1883, **14**, 170–177.

3 G. Taylor, *Proc. R. Soc. Lond. A.*, 1950, **201**, 192–196.

4 L. Rayleigh, *Proc. Lond. Math. Soc.*, 1878, **1**, 4–13.

5 S. Mora, T. Phou, J.-M. Fromental and Y. Pomeau, *Phys. Rev. Lett.*, 2014, **113**, 178301.

6 S. Mora, T. Phou, J.-M. Fromental, L. M. Pismen and Y. Pomeau, *Phys. Rev. Lett.*, 2010, **105**, 214301.

7 P. Ciarletta and M. B. Amar, *Soft Matter*, 2012, **8**, 1760–1763.

8 C. Xuan and J. Biggins, *Phys. Rev. E*, 2017, **95**, 053106.

9 B. Saintyves, O. Dauchot and E. Bouchaud, *Phys. Rev. Lett.*, 2013, **111**, 047801.

10 J. S. Biggins, B. Saintyves, Z. Wei, E. Bouchaud and L. Mahadevan, *Proc. Natl. Acad. Sci. (USA)*, 2013, **110**, 12545–12548.

11 J. Bataille, *Revue Inst. Pétrole*, 1968, **23**, 1349–1364.

12 K. Shull, C. Flanigan and A. Crosby, *Phys. Rev. Lett.*, 2000, **84**, 3057–3060.

13 Q. Liu, Z. Wang, Y. Lou and Z. Suo, *Extreme Mech. Lett.*, 2014, **1**, 54–61.

14 J. Nittman, G. Daccord and M. Stanley, *Nature*, 1985, **314**, 391.

15 H. Van Damme, F. Obrecht, P. Levitz, L. Gatineau and C. Laroche, *Nature*, 1986.

16 A. Lindner, D. Bonn, E. C. Poiré, M. B. Amar and J. Meunier, *J. Fluid Mech.*, 2002, **469**, 237–256.

17 S. Wilson, *J. Fluid Mech.*, 1990, **220**, 413–425.

18 H. Zhao and J. Maher, *Phys. Rev. E*, 1993, **47**, 4278.

19 T. Hirata, *Phys. Rev. E*, 1998, **57**, 1772.

20 E. Lemaire, P. Levitz, G. Daccord and H. Van Damme, *Phys. Rev. Lett.*, 1991, **67**, 2009.

21 S. Mora and M. Manna, *J. Nonnewton. Fluid Mech.*, 2012, **173**, 30–39.

22 S. Mora and M. Manna, *Phys. Rev. E*, 2010, **81**, 026305.

23 J. Nase, A. Lindner and C. Creton, *Phys. Rev. Lett.*, 2008, **101**, 074503.

24 M. B. Amar and E. C. Poiré, *Phys. Fluids (1994-present)*, 1999, **11**, 1757–1767.

25 L. Kondic, M. J. Shelley and P. Palffy-Muhoray, *Phys. Rev. Lett.*, 1998, **80**, 1433.

26 P. Coussot, *J. Fluid Mech.*, 1999, **380**, 363–376.

27 A. Lindner, P. Coussot and D. Bonn, *Phys. Rev. Lett.*, 2000, **85**, 314.

28 T. Podgorski, M. C. Sostarecz, S. Zorman and A. Belmonte, *Phys, Rev. E*, 2007, **76**, 016202.

29 A. He, J. Lowengrub and A. Belmonte, *SIAM J. Appl. Math.*, 2012, **72**, 842–856.

30 G. D. Carvalho, J. A. Miranda and H. Gadêlha, *Phys. Rev. E*, 2013, **88**, 053006.

31 A. Gent and P. Lindley, *Proc. R. Soc. Lond. A*, 1959, **249**, 195–205.

32 S. Lin, T. Cohen, T. Zhang, H. Yuk, R. Abeyaratne and X. Zhao, *Soft matter*, 2016, **12**, 8899–8906.

33 S. Lin, Y. Mao, H. Yuk and X. Zhao, *Int. J. Solids Struct.*, 2018.

34 A. Ghatak and M. K. Chaudhury, *Langmuir*, 2003, **19**, 2621–2631.

35 A. Ghatak, L. Mahadevan, J. Y. Chung, M. K. Chaudhury and V. Shenoy, *Proc. R. Soc. Lond. A*, 2004, **460**, 2725–2735.

36 M. Adda-Bedia and L. Mahadevan, *Proc. R. Soc. Lond. A*, 2006, **462**, 3233–3251.

37 T. Vilmin, F. Ziebert and E. RaphaÃńl, *Langmuir*, 2010, **26**, 3257–3260.

38 M. K. Chaudhury, A. Chakrabarti and A. Ghatak, *Eur. Phys. J. E*, 2015, **38**, 82.

39 Z. Wei and L. Mahadevan, *Soft matter*, 2016, **12**, 1778–1782.

40 B. Mukherjee, R. C. Batra and D. A. Dillard, *Int. J. Solids Struct*, 2017, **110**, 385–403.

41 S. Lin, Y. Mao, R. Radovitzky and X. Zhao, *J. Mech. Phys. Solids*, 2017, **106**, 229–256.

42 J. Biggins, Z. Wei and L. Mahadevan, *Europhys. Lett.*, 2015, **110**, 34001.

43 A. Flamant, *CR Acad. Sci. Paris*, 1892, **114**, 1465–1468.

44 M. Levy, *C.R. Acad. Sci. Paris*, 1899, **126**, 1235–1240.